A Low-dimensional Step Pattern Analysis Algorithm with Application to Multimodal Retinal Image Registration

Jimmy Addison Lee[1], Jun Cheng[1], Beng Hai Lee[1], Ee Ping Ong[1], Guozhen Xu[1], Damon Wing Kee Wong[1], Jiang Liu[1], Augustinus Laude[2], Tock Han Lim[2]

[1]Institute for Infocomm Research (I²R), Agency for Science, Technology and Research (A*STAR), Singapore. [2]National Healthcare Group, Eye Institute, Tan Tock Seng Hospital, Singapore.

Retinal image registration is increasingly important for assisting ophthalmologists in diagnosis and treatment of various eye diseases. This paper focuses on the registration group of aligning images of different modalities captured by different sensors to obtain a more complete detail of the subject. The main challenges in this registration group are the non-linear intensity differences between two modalities and the poor quality of the multimodal retinal images which are adversely affected by pathologies or noise.

In this paper, we aim to design a registration algorithm which comes with a low-dimensional descriptor that is invariant to linear and non-linear intensity changes, and provides sufficient distinctiveness to register unhealthy multimodal retinal image pairs. We first exploit the geometric corner extraction method [3] in our previous paper to locate hypotheses of robust corner features based on connecting edges from the edge maps of the multimodal retinal images. Next, we rotate the extracted corner features to a mutual orientation to achieve rotation invariance. Given each pair of connecting edges $\ell_1^{g_i}$ and $\ell_2^{g_i}$ and the center of rotation at g_i, the angle-to-rotate $\theta_{rot}^{g_i}$ is derived as follows

$$\theta_{rot}^{g_i} = \theta_{min}^{g_i} + [\delta]\,(\theta_{max}^{g_i} - \theta_{min}^{g_i}), \tag{1}$$

where $\theta_{max}^{g_i}$ and $\theta_{min}^{g_i}$ denote the maximum and minimum angles from $\ell_j^{g_i}$ to the positive x-axis respectively, with $\forall j \in \{1,2\}$. $[.]$ is a binary indicator function, and δ is the inequality formalized as:

$$\theta_{max}^{g_i} - \theta_{min}^{g_i} > 180^\circ. \tag{2}$$

After rotation, we extract a local window $\mathbf{W}_{rot}^{g_i}$ (e.g. 15×15) centered at g_i from the rotated image. We propose to divide $\mathbf{W}_{rot}^{g_i}$ into equal-sized subregions using two straight lines. We then compare the average intensities between the subregions, which will be computed as a feature representation for $\mathbf{W}_{rot}^{g_i}$. 28 different patterns are empirically proposed, which represent most of the possible patterns with equal-sized subregions as shown in Fig. 1 and 2. The patterns are called step patterns. As the name implies, these patterns come in step forms of two to four height levels where the higher level steps indicate subregions of higher average intensity values. Taking Fig. 1(c) as an exemplar with subregions from left to right denoted as $\mathbf{R_1}$, $\mathbf{R_2}$ and $\mathbf{R_3}$ respectively, the number of pixels in the subregions are equal. For average intensity value $I_{avg}^{\mathbf{R_k}}$ in $\mathbf{R_k}$ where $\forall \mathbf{k} \in \{1,2,3\}$, we formulate as follows:

$$I_{avg}^{\mathbf{R_k}} = \frac{1}{N} \sum_{(x,y)\in\mathbf{R_k}} \mathbf{W}_{rot}^{g_i}(x,y), \tag{3}$$

where N is the number of pixels in $\mathbf{R_k}$. Each $\mathbf{W}_{rot}^{g_i}$, in relation with its respective g_i, can be described using the equation:

$$d_1 = \left[I_{avg}^{\mathbf{R_1}} - I_{avg}^{\mathbf{R_2}} > \tau\right] \cdot \left[I_{avg}^{\mathbf{R_3}} - I_{avg}^{\mathbf{R_2}} > \tau\right], \tag{4}$$

where d_1 is a binary result to indicate the existence of the step pattern in Fig. 1(c), and τ denotes a position integer value. To deal with contrast reversal problem such as the change in intensities between the local neighborhood of two image modalities (for instance, some dark vessels become bright), the step pattern is reversible. Hence, the equation for the reversed step pattern can be rearranged as:

$$d_2 = \left[I_{avg}^{\mathbf{R_2}} - I_{avg}^{\mathbf{R_1}} > \tau\right] \cdot \left[I_{avg}^{\mathbf{R_2}} - I_{avg}^{\mathbf{R_3}} > \tau\right]. \tag{5}$$

The final equation to describe $\mathbf{W}_{rot}^{g_i}$ is given by:

$$d_3 = d_1 + d_2. \tag{6}$$

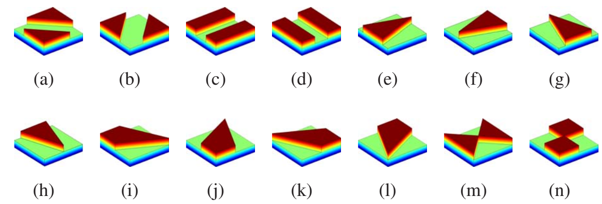

Figure 1: Two-level step patterns.

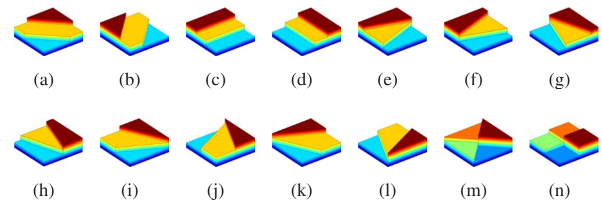

Figure 2: Three- and four-level step patterns.

In order to describe the inner and outer regions of the local neighborhood surrounding g_i, two $\mathbf{W}_{rot}^{g_i}$ of different scales are deployed each time. We also include the angle between $\ell_1^{g_i}$ and $\ell_2^{g_i}$, and the angle-to-rotate $\theta_{rot}^{g_i}$. It sums up to a 58-dimensional. For improved robustness to scale changes, we also include a version with an additional window scale of 27×27 in our experiment, resulting in a 86-dimensional $(28\times3+2)$ LoSPA feature vector. We tagged the two versions as LoSPA-58 and LoSPA-86 accordingly. We find matches by Euclidean distance using the k-dimensional data structure and search algorithm [1], and exploit affine model [2] as the transformation function in our framework. When it has been applied on the floating retinal image, we simply superpose the transformed retinal image on the fixed retinal image to produce a retinal mosaic as shown in Fig. 3.

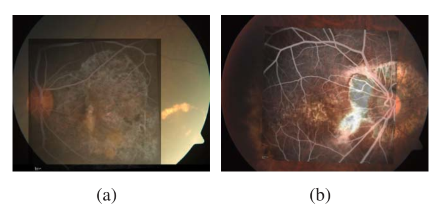

Figure 3: Mosaic results of the proposed algorithm (LoSPA-86).

In our experiments, the LoSPA-58 and LoSPA-86 algorithms outperformed existing algorithms in term of root-mean-square-error (RMSE), median error (MEE) and maximal error (MAE) in two datasets, one of mild-to-moderate diseases and the other of severe diseases. On the severe disease dataset, LoSPA-86 achieved close to two-fold higher in registration success rate than the top score among the state-of-the-art algorithms.

[1] J. L. Bentley. Multidimensional binary search trees used for associative searching. *Comm. ACM*, 18(9):509–517, 1975.

[2] R. Jagoe, C. I. Blauth, P. L. Smith, J. V. Smith, J. V. Arnold, K. Taylor, and R. Wootton. Automatic geometrical registration of fluorescein retinal angiograms. *Comp. and Biomed. Research*, 23(5):403–409, 1990.

[3] J. A. Lee, B. H. Lee, G. Xu, E. P. Ong, D. W. K. Wong, J. Liu, and T. H. Lim. Geometric corner extraction in retinal fundus images. In *Proc. EMBC*, 2014.